

2-D ZO CRS stack by considering an acquisition line with smooth topography

P. Chira-Oliva, J.C.R. Cruz, G. Garabito, P. Hubral, and M. Tygel

email: *chira@ufpa.br*

keywords: *CRS stack, smooth topography, measurement surface curvature, near-surface irregularities*

ABSTRACT

The land seismic data suffers from effects due to the near surface irregularities and the existence of topography. For obtaining a high resolution seismic image, these effects should be corrected by using seismic processing techniques, e.g. field and residual static corrections. The Common-Reflection-Surface (CRS) stack method is a new processing technique to simulate zero-offset (ZO) seismic sections from multi-coverage seismic data. It is based on a second-order hyperbolic paraxial traveltimes approximation referred to a central normal ray. By considering a planar measurement surface, the CRS stacking operator is defined by means of three parameters, namely the emergence angle of the normal ray, the curvature of the normal incidence point (NIP) wave, and the curvature of the normal (N) wave. In this paper the 2-D ZO CRS stack method is modified in order to consider effects due to the smooth topography. By means of this new CRS formalism, we obtain a high resolution ZO seismic section, without applying static corrections. As by-products the 2-D ZO CRS stack method we estimate at each point of the ZO seismic section the three relevant parameters associated to the CRS stack process.

INTRODUCTION

In order to obtain a high-resolution image of the earth sub-surface the geophysicists use the multi-coverage seismic data acquisition, that yields to overlap registers of geological targets. In time domain, the ZO section is the seismic image obtained by considering coincident sources and receivers. This is simulated by stacking the amplitudes using a traveltimes operator, which is defined by means of stack parameters.

By the conventional seismic processing, the ZO section is simulated using the well-known normal moveout/dip moveout (NMO/DMO) stack method. Mann et al. (1999) presented a new stack method, so-called Common-Reflection-Surface (CRS), based on a hyperbolic second-order paraxial approach. By considering a planar measurement surface, it depends on three parameters, namely, the emergence angle β_o of the normal ray, the curvatures K_{NIP} and K_N of the two hypothetical wavefront, so-called NIP and N waves, respectively (Hubral, 1983).

Land seismic data are in general affected by the existence of surface topography and irregularities in the near-surface (e.g. weathering base and weathering velocity). In the conventional seismic processing, these effects are interpreted by deviations from hyperbolic NMO correction in the common-midpoint (CMP) gather. The topography effects are corrected by using field and residual static corrections. By applying specifically the field static correction, based on refraction seismic data, we remove the most part of these traveltimes anomalies. Nevertheless, this correction usually does not account for rapid changes of the topography, in the weathering base, and of the weathering velocity. It is very sensitive to the choice of parameters involved in the picking phase.

According to Guo and Fagin (2002), land surveys should always be processed considering a floating datum that represents the topography. They showed that velocity analysis from a flat seismic reference datum creates errors to estimate the depth and interval velocities, even in the case of a flat topography, due to deviations of the take-off angles of the seismic ray paths.

Chira-Oliva and Hubral (2003) studied the sensibility of the interval velocity and reflector depth by considering a hypothetical circle measurement surface. They showed the NMO velocity by considering the curvature of the earth surface is more accurate to recover the interval velocities and the depths of the reflectors than the NMO velocities obtained by using a planar measurement surface approach. Chira-Oliva and Hubral (2003) and Zhang et al. (2002), respectively, presented the 2-D ZO CRS formalism for measurement surface with smooth and rugged topography. Chira-Oliva et al. (2001) modified the 2-D ZO CRS operator for including effects of near-surface inhomogeneity. In this paper, the 2-D ZO CRS stack performance is tested by considering a multi-layer model with smooth topography.

THEORY

The 2-D ZO CRS stacking operator depends on three parameters of two hypothetical waves, namely the normal-incidence-point (NIP) and Normal (N) waves (Hubral, 1983). These parameters are the emergence angle of the normal ray, and the radii of curvatures of the NIP and N waves. The emergence point, X_0 , of the normal ray is called central point. The NIP wave propagates upwards from a point source located at the normal ray incidence point; and the N wave propagates upwards starting at the reflector, like an exploding reflector source.

Based on the hyperbolic second-order paraxial travelttime approach, the 2-D ZO CRS stacking operator with smooth topography is given by (Chira-Oliva et al. (2001))

$$t^2(x_m, h) = \left(t_0 + 2 \frac{\sin \beta_0^*}{v_1} (x_m - x_0) \right)^2 + \frac{2 t_0}{v_1} \left(\frac{\cos^2 \beta_0^*}{R_N} - \cos \beta_0^* K_0 \right) (x_m - x_0)^2 + \frac{2 t_0}{v_1} \left(\frac{\cos^2 \beta_0^*}{R_{NIP}} - \cos \beta_0^* K_0 \right) h^2. \quad (1)$$

Equation (1) describes the reflection time t of the paraxial ray SPG in the vicinity of a normal (ZO) ray X_0 NIP X_0 (Figure 1a). The ZO travel-time and the central point coordinate are t_0 and x_0 , and v_1 is the near-surface velocity of the P-P wave at the central point X_0 . The coordinates x_m and h are, respectively, the midpoint and half-offset referred to the x_1 -axis, that is tangent to the topography surface with origin at the central point X_0 (see Figures 1a,b). The emergence angle of the normal ray at the central point is β_0^* . The parameter K_0 is the local curvature of the earth surface at a point of the acquisition line, that is positive (or negative) if this line falls below (or above) its tangent at X_0 . The radii of curvatures of the emergence hypothetical NIP and N wavefronts at X_0 are R_{NIP} and R_N respectively.

In order to normalize the processing coordinates, we apply a transformation from the local (x_1, x_3) into the global cartesian system (x, z) in Figure 1b. The midpoint and half-offset coordinates, (x_m, h) and (x'_m, h') , in the local and global coordinate cartesian systems, respectively, are related by the expressions

$$h = \frac{h'}{\cos \alpha_0^*}, \quad x_m = \frac{x'_m}{\cos \alpha_0^*}, \quad (2)$$

where α_0^* is the dip angle of the tangent x_1 -axis at point X_0 . Introducing the relationships (2) into equation (1), we find (Chira-Oliva and Hubral, 2003; Chira, 2003)

$$t^2(x'_m, h') = \left(t_0 + 2 \frac{\sin \beta_0^*}{v_1 \cos \alpha_0^*} (x'_m - x_0) \right)^2 + \frac{2 t_0}{v_1 \cos^2 \alpha_0^*} \left(\frac{\cos^2 \beta_0^*}{R_N} - \cos \beta_0^* K_0 \right) (x'_m - x_0)^2 + \frac{2 t_0}{v_1 \cos^2 \alpha_0^*} \left(\frac{\cos^2 \beta_0^*}{R_{NIP}} - \cos \beta_0^* K_0 \right) (h')^2. \quad (3)$$

We now consider a *pure diffraction*, i.e., the situation in which the reflector reduces to a single diffraction point. In this case, the NIP and N waves are coincident, i.e. both propagate from a point source at NIP and have identical radii of curvatures at X_0 , $R_N \equiv R_{NIP}$. As a consequence, equation (3) becomes

$$t_{diff}^2(x'_m, h') = \left(t_0 + 2 \frac{\sin \beta_0^*}{v_1 \cos \alpha_0^*} (x'_m - x_0) \right)^2 + \frac{2 t_0}{v_1 \cos^2 \alpha_0^*} \left(\frac{\cos^2 \beta_0^*}{R_{NIP}} - \cos \beta_0^* K_0 \right) ((x'_m - x_0)^2 + (h')^2). \quad (4)$$

Equation (4) depends on two CRS parameters (R_{NIP}, β_0^*) associated to the NIP wave. This equation will be used at the first step of the CRS strategy. The CRS stacking operator defined by equation (4) is interpreted as an approach of the pre-stack Kirchhoff migration operator with smooth topography.

Setting the condition $h' = 0$ to the general hyperbolic travel-time equation (3), the CRS stacking operator for reflected events in the ZO configuration becomes

$$t_{ZO}^2(x'_m) = \left(t_0 + 2 \frac{\sin \beta_0^*}{v_1 \cos \alpha_0^*} (x'_m - x_0) \right)^2 + \frac{2 t_0}{v_1 \cos^2 \alpha_0^*} \left(\frac{\cos^2 \beta_0^*}{R_N} - \cos \beta_0^* K_0 \right) (x'_m - x_0)^2. \quad (5)$$

Following Garabito et al. (2001) the three optimal CRS parameters $(\beta_0^*, R_{NIP}, R_N)$ are searched by three steps. At the first step we use formula (4) to determine β_0^* and R_{NIP} . At the second step we use formula (5) to determine R_N ; and at the third step we use formula (3) to refine the three parameters.

2-D ZO CRS STACK

In the 2-D situation, for each point $P_0(x_0, t_0)$ at the ZO section to be simulated, the amplitudes in the seismic data will be summed (stacked) along the CRS surface defined by equation (3). The resulting (stacked) amplitude is assigned to the point P_0 .

The three CRS stacking parameters are estimated by means of an optimization process, having the semblance as objective function. The CRS stacking optimization problem consists of estimating the parameters that maximize the semblance. In general, the problem requires a combination of multi-dimensional global and local optimization algorithms. The mathematical intervals defined for the parameters are $-\pi/2 < \beta_0^* < \pi/2$, $-\infty < R_{NIP}, R_N < \infty$. Optimization strategies to estimate these parameters are found in the literature (e.g. Müller (1999); Birgin et al. (1999); Garabito et al. (2001)).

In this paper, we apply the strategy given by Garabito et al. (2001) to estimate the CRS parameters triplet, but using the new equations (3), (4) and (5).

CRS STACK PROCESSING STRATEGY

The proposed strategy to carry out the CRS method involves a combination of global and local search processes and is divided into three steps. The curvature, K_0 , of the seismic line at each central point is supposed to be a priori known or calculated by means of some interpolation method by using elevation values. At the first and second steps we used the Simulated Annealing (SA) algorithm (Sen and Stoffa, 1995), and at the third step the Quasi-Newton (QN) algorithm (Bard (1974); Gill et al. (1981)). Each step is performed on each sample point $P_0(x_0, t_0)$ that pertains to the ZO section to be simulated. The objective function is the semblance calculated for each point in the ZO section.

Step I : Pre-Stack Global Optimization The multi-coverage pre-stack seismic data is the input. The inverse problem consists of simultaneously estimating the two parameters β_0^* and R_{NIP} that provide the maximum semblance value, according equation (4). The results of this step are: 1) maximum coherence section, 2) emergence angle, β_0^* - section, 3)NIP-wave radius of curvature, R_{NIP} -section, and 4)simulated (stacked) ZO section.

Step II : Post-Stack Global Optimization The post-stack seismic data is the input. The inverse problem consists of estimating the single parameter, R_N , that provides the maximum semblance according to equation (5), in which the previously obtained parameter, β_0^* , is kept fixed. In this step the results are: 1)

maximum coherence section, 2)N-wave radius of curvature, R_N -section, and 3)re-stacked simulated ZO (stacked) section.

Step III : Pre-Stack Local Optimization The multi-coverage pre-stack seismic data from step I is the input. The inverse problem consists of estimating the best parameter triplet $(\beta_0^*, R_{NIP}, R_N)$ that provides the maximum semblance. In this case the CRS stacking operator is equation (3), applied to the full multi-coverage data set with suitable apertures. In this step the results are: 1) maximum coherence section, 2) optimized β_0^* -section, 3)optimized R_{NIP} -section, 4)optimized R_N -section, and 5)optimized ZO (stacked) section.

Example

In order to test the CRS stacking algorithm we applied it to a synthetic data set computed for 2-D homogeneous layered model shown in Figure 2. The model is constituted of four layers above a half-space. The acquisition system is lying on a smooth topography line. Based on this model, we generated a synthetic data set of multi-coverage primary reflections, using the ray-tracing algorithm, SEIS88 (Červený and Pseník, 1988). In order to test the accuracy of the CRS method, it was added random noise with signal-to-noise ratio of $S/N = 10$. The data set consisted of 201 common-shots (CS) with 72 receivers with interval of 50 meters. The minimum offset was 50 meters. The source signal was a Gabor wavelet with 40 Hz dominant frequency and the time sampling was 4 ms. An example of part of these data is presented in Figure 3, represented by a CS section.

Figure 4 shows the ray-theoretical modelled ZO section with random noise added. Figure 5 shows the simulated ZO section that results from the application of the CRS stack method for a curved measurement surface. Due to the fact that the CRS method involves a larger number of traces during the stacking process, the simulated ZO section presents enhanced primary reflection events, with larger signal-to-noise ratio than the corresponding ones in the modelled ZO section (Figure 4). Figure 6 shows the maximum coherence (semblance) section that corresponds to the best parameters. We note that the coherence values become smaller for larger traveltimes (deeper events). Figures 7, 8 and 9 show the sections of emergence angle and radii of curvature of the NIP and N waves, respectively. These sections correspond to global maxima determined at the third step.

A comparison between the emergence angles, β_0^* , estimated by the CRS algorithm (curves of red points) and by modelling (curves of blue points), respectively, is shown in Figure 10. We can see the emergence angle has been well estimated along all reflectors. Figures 11 and 12 show the analogous comparison for the other parameters, R_{NIP} e R_N , respectively. These parameters are also well estimated, with the exception of the locations where abrupt changes of the curvature K_0 are present (Figure 13).

CONCLUSIONS

A new formula for the CRS stack method that considers the smooth topography of the acquisition line has been tested in synthetic data sets with successful results. The parameters were correctly estimated, excepting the regions where there are abrupt changes of the curvature of the topography line. In these regions, the errors of the estimated parameters increase with depth. Besides the simulated ZO sections, we have obtained the coherence section and the sections referred to the attributes of the NIP and N waves.

ACKNOWLEDGMENTS

We thank the financial support in part by the IMAGAM Project of the CTPETRO/FINEP/CNPq/UFGA. The first author also thanks to the National Council of Technology and Development (CNPq), Brazil, for the scholarship, and to the sponsors of the Wave Inversion Technology (WIT) Consortium (Germany) for their support.

REFERENCES

- Bard, B. (1974). *Nonlinear parameter estimation: Academic Press.*
- Birgin, E. G., Biloti, R., Tygel, M., and Santos, L. (1999). Restricted optimization: a clue to a fast

- and accurate implementation of the common reflection surface stack. *Journal of Applied Geophysics*, 42:143–155.
- Červený, V. and Psensik, I. (1988). Ray tracing program. *Charles University, Czechoslovakia*.
- Chira, P. (2003). Empilhamento pelo método Superfície de Reflexão Comum 2-D com topografia e introdução ao caso 3-D. *Ph.D. thesis, Federal University of Pará, Brazil (in Portuguese)*.
- Chira-Oliva, P. and Hubral, P. (2003). Traveltime formulas of near-zero-offset primary reflections for a curved 2-D measurement surface. *Geophysics*, 68(1):255–261.
- Chira-Oliva, P., Tygel, M., Zhang, Y., and Hubral, P. (2001). Analytic CRS stack formula for a 2D curved measurement surface and finite-offset reflections. *Journal of Seismic Exploration*, 10:245–262.
- Garabito, G., Cruz, J. C., Hubral, P., and Costa, J. (2001). Common reflection surface stack: A new parameter search strategy by global optimization. *71th. SEG Mtg., Expanded Abstracts. San Antonio, Texas, USA*.
- Gill, P. E., Murray, W., and Wright, M. H. (1981). *Practical optimization: Academic Press*.
- Guo, N. and Fagin, S. (2002). Becoming effective velocity-model builders and depth imagers, part 2 - the basics of velocity-model building, examples and discussionsmultifocusing. *The Leading Edge*, pages 1210–1216.
- Hubral, P. (1983). Computing true amplitude reflections in a laterally inhomogeneous earth. *Geophysics*, 48:1051–1062.
- Mann, J., Jäger, R., Müller, T., Höcht, G., and Hubral, P. (1999). Common-reflection-surface stack - a real data example. *Journal of Applied Geophysics*, 42:301–318.
- Müller, T. (1999). The common reflection surface stack method - seismic imaging without explicit knowledge of the velocity model. *Ph.D. Thesis, University of Karlsruhe, Germany*.
- Sen, M. and Stoffa, P. (1995). Global optimization methods in geophysical inversion. *Elsevier, Science Publ. Co.*
- Zhang, Y., Höcht, G., and Hubral, P. (2002). 2D and 3D ZO CRS stack for a complex top-surface topography. *Expanded Abstract of the 64th EAGE Conference and Technical Exhibition*.

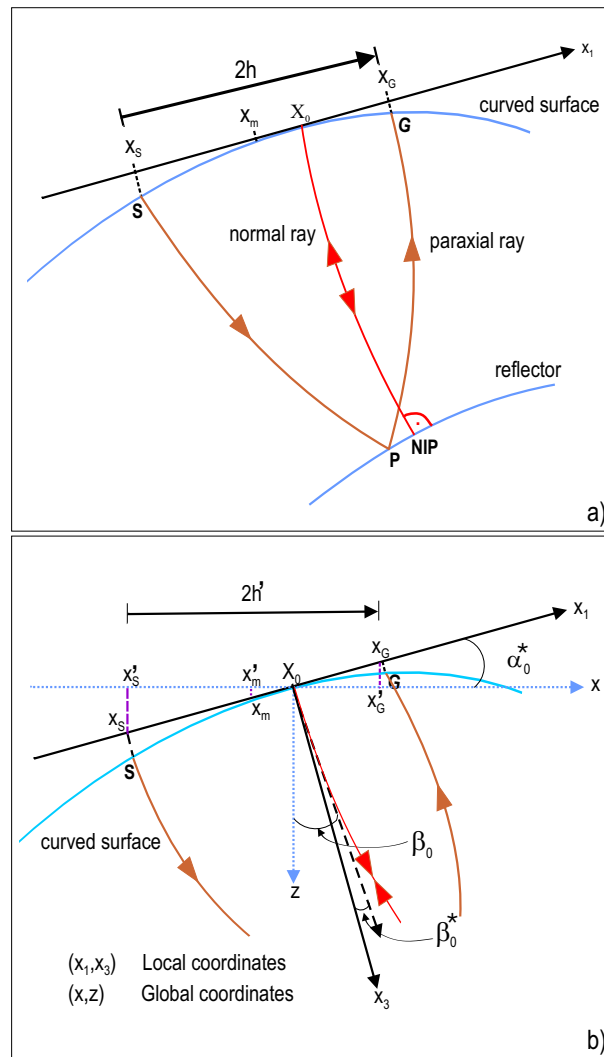


Figure 1: a) Ray diagram for a paraxial ray in the vicinity of a normal ray in a 2-D laterally inhomogeneous medium. Local coordinates system (x_1, x_3) for a curved measurement surface referred to point X_0 . b) Transformation of the local coordinates, x_m and h , to its global coordinates x_m' and h' . The local dip angle of the tangent at X_0 (x_1 -axis) is defined by α_0^* . The angle between the normal ray and the vertical line through X_0 (z -axis) is β_0 , and β_0^* is the angle between the normal ray and the normal to the tangent at X_0 .

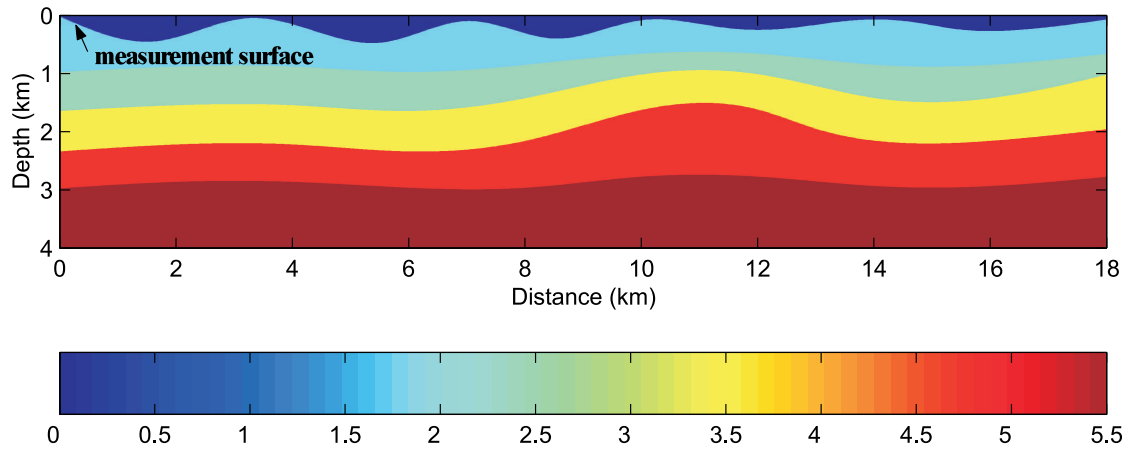


Figure 2: 2-D model constituted of four isovelocity layers about a half-space with curved interfaces and curved measurement surface. Interval velocities are 1.75 km/s, 2.4 km/s, 3.5 km/s, 4.65 km/s and 5.5 km/s, respectively.

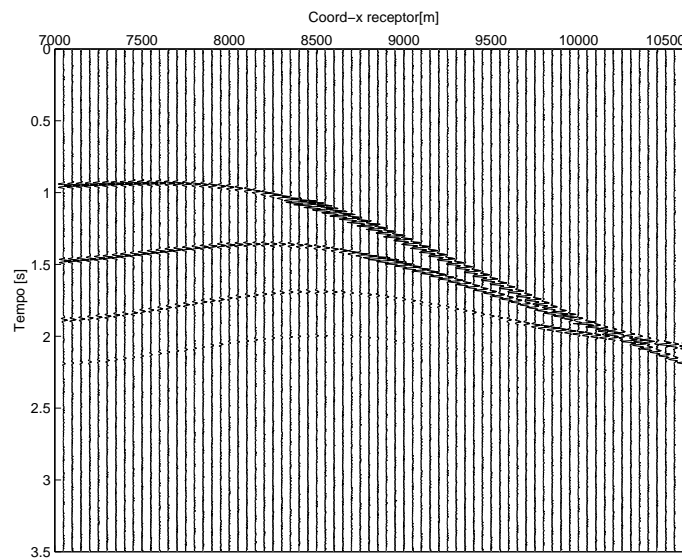


Figure 3: Example of a CS section of multi-coverage pre-stack seismic data of the model of Figure 2. The ratio signal/noise is 10.

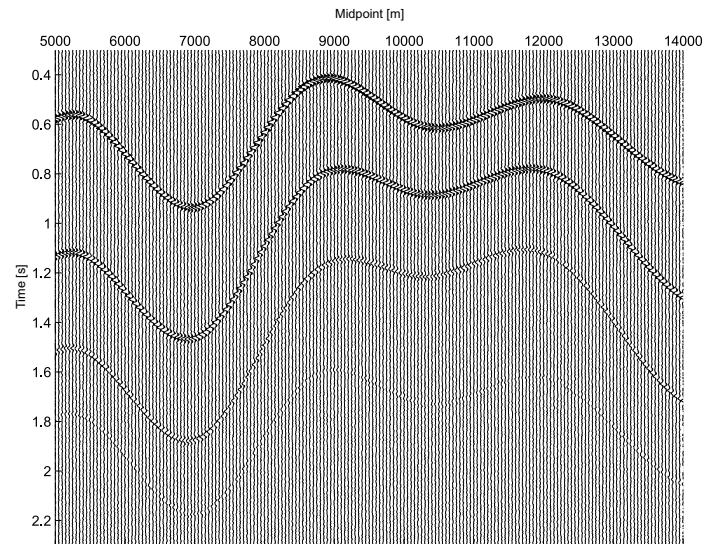


Figure 4: ZO section with random noise (ratio $S/N = 10$) obtained by forward modelling.

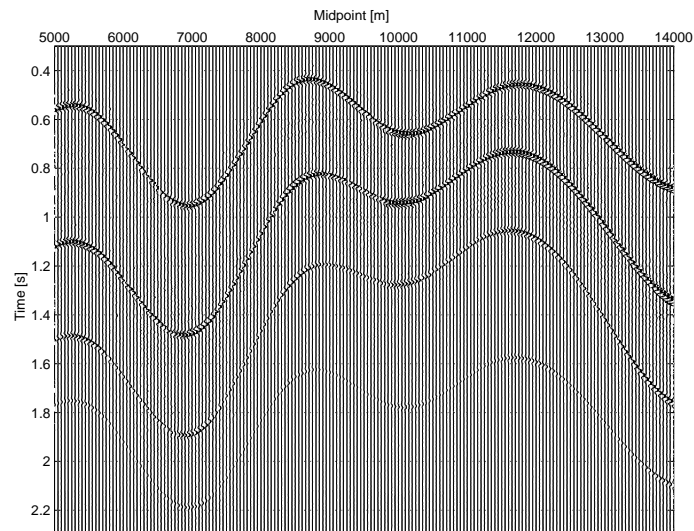


Figure 5: Simulated ZO section with the ZO CRS stack by using the multi-coverage seismic data with random noise (ratio $S/N = 10$).

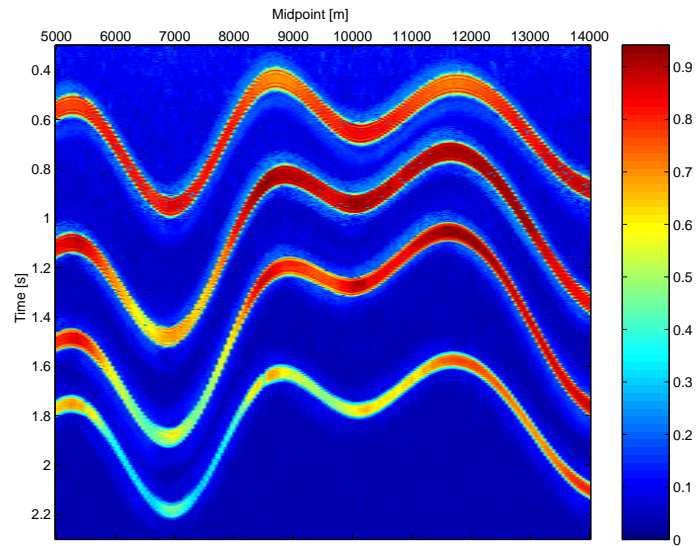


Figure 6: CRS optimized coherence section of the model of Figure 2.

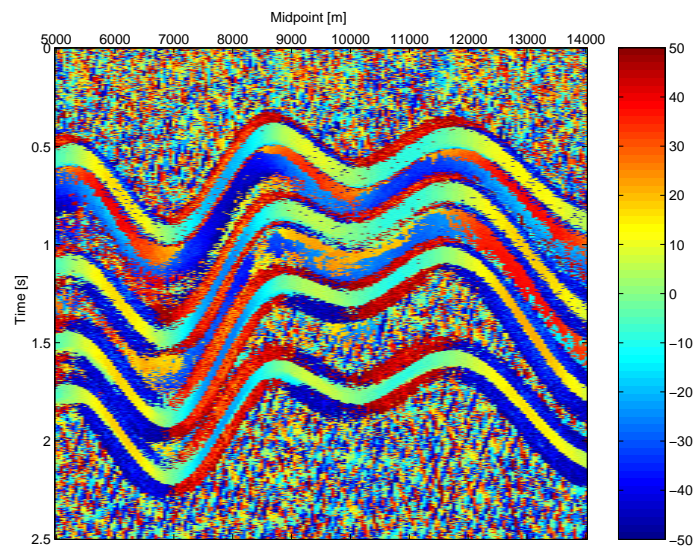


Figure 7: CRS optimized β_0^* -section of the model of Figure 2.

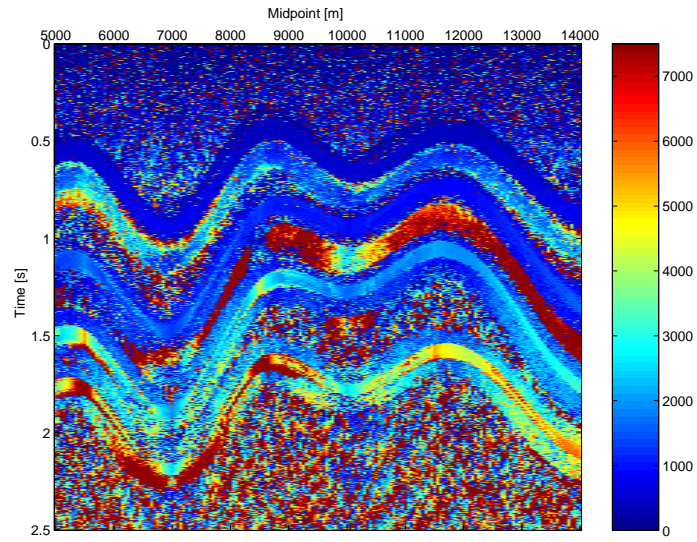


Figure 8: CRS optimized R_{NIP} -section of the model of Figure 2.

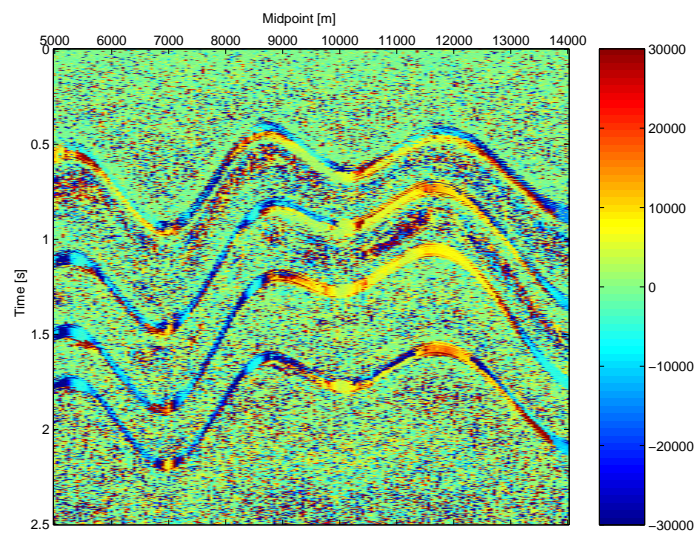


Figure 9: CRS optimized R_N -section of the model of Figure 2.

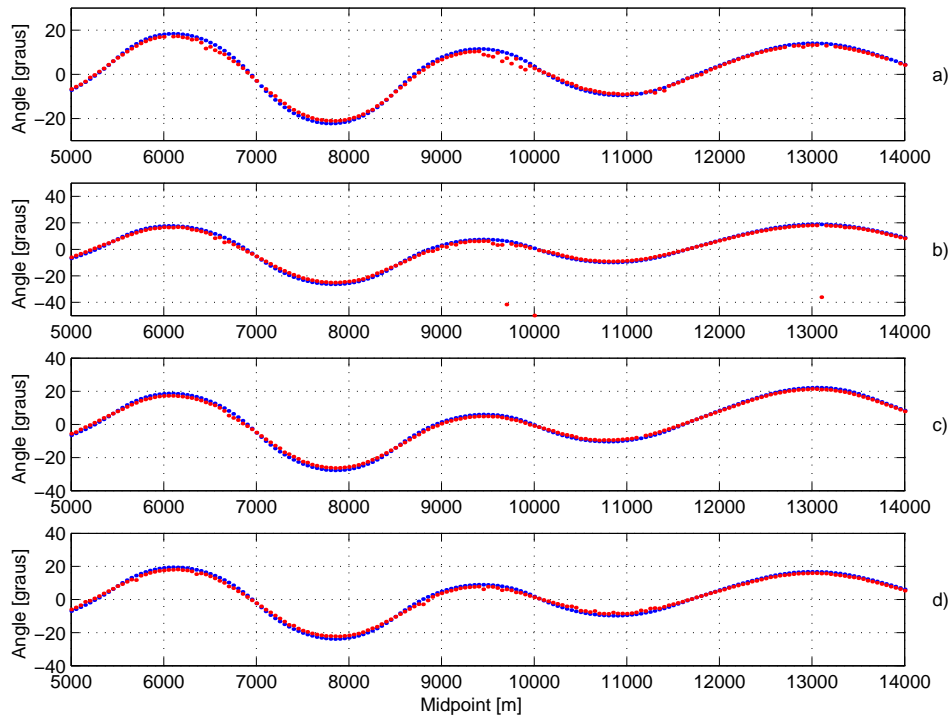


Figure 10: Comparison between CRS (curve of red points) and model-derived (curve of blue points) emergence angles β_0^* . The parameter for each interface are plotted separately: a) first, b) second, c) third and d) fourth interface of the model of Figure 2.

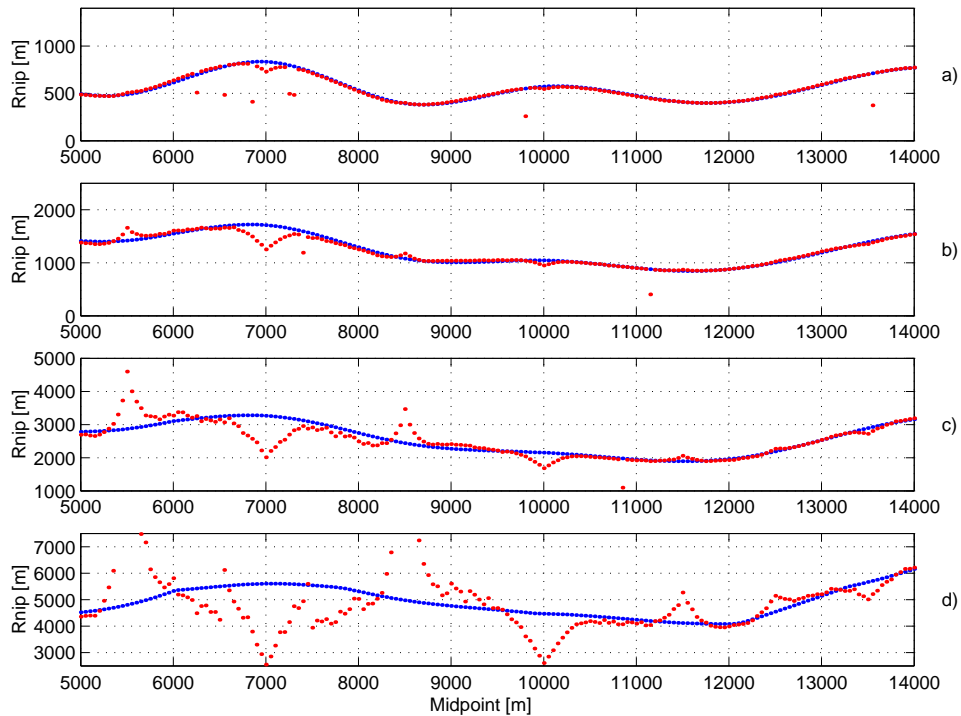


Figure 11: Comparison between CRS (curve of red points) and model-derived (curve of blue points) radius of curvature, R_{NIP} . The parameter for each interface are plotted separately: a) first, b) second, c) third and d) fourth interface of the model of Figure 2.

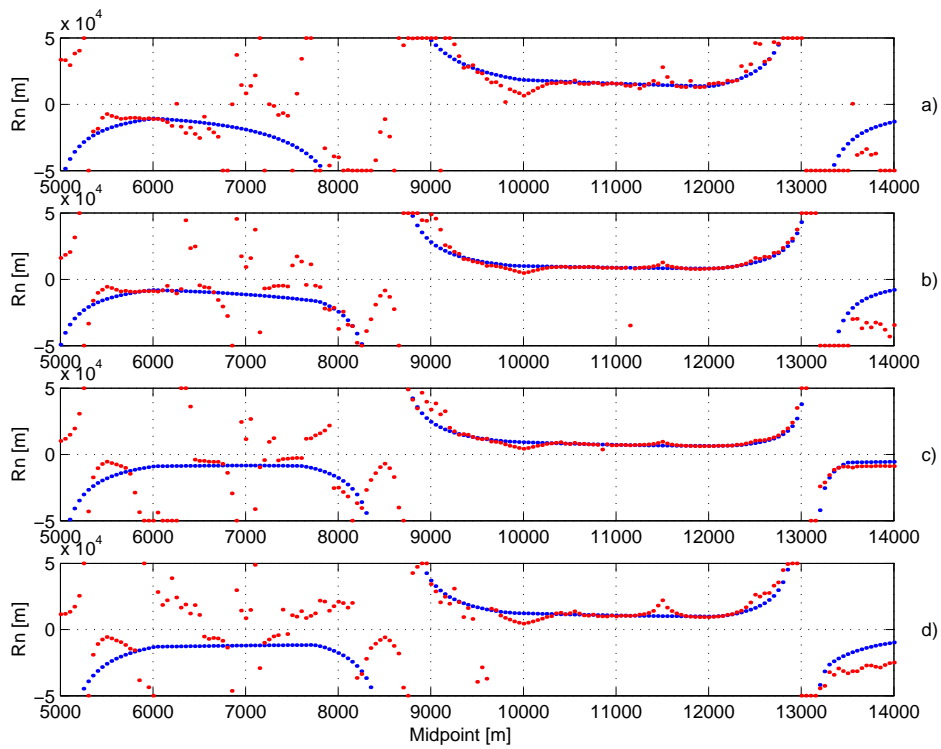


Figure 12: Comparison between CRS (curve of red points) and model-derived (curve of blue points) radius of curvature, R_N . The parameter for each interface are plotted separately: a) first, b) second, c) third and d) fourth interface of the model of Figure 2.

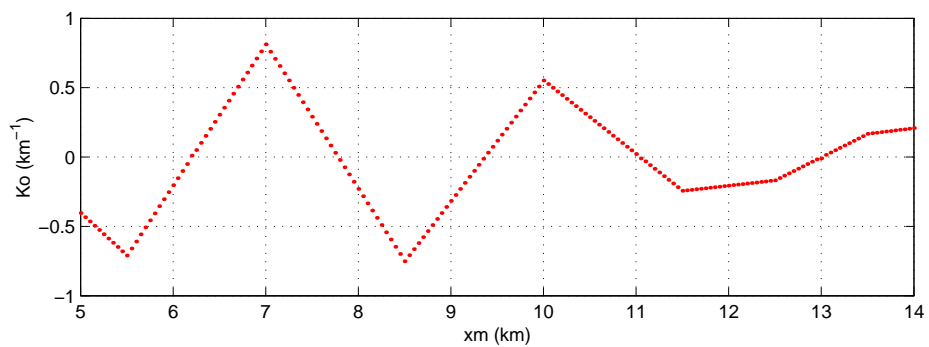


Figure 13: Curvature of measurement surface along the acquisition line. It presents the points of abrupt changes of the curvature of the model of Figure 2.